ATP Augments von Willebrand Factor-dependent Shear-induced Platelet Aggregation through Ca^{2+}-Calmodulin and Myosin Light Chain Kinase Activation*

Cécile Oury‡§, Elsie Sticker‡, Heidi Cornelissen‡, Rita De Vos¶, Jos Vermylen‡, and Marc F. Hoylaerts‡||

From the ‡Center for Molecular and Vascular Biology and the ¶Laboratory of Morphology and Molecular Pathology, University of Leuven, 3000 Leuven, Belgium

Shear stress triggers von Willebrand factor (VWF) binding to platelet glycoprotein Ibα and subsequent integrin $\alpha_{IIb}\beta_3$-dependent platelet aggregation. Concomitantly, nucleotides are released from platelet-dense granules, and ADP is known to contribute to shear-induced platelet aggregation (SIPA). We found that the impaired SIPA of platelets from a Hermansky-Pudlak patient lacking dense granules was restored by exogenous L-β,γ-methylene ATP, a stable P2X$_1$ agonist, as well as by ADP, confirming that in addition to ADP (via P2Y$_1$ and P2Y$_{12}$), ATP (via P2X$_1$) also contributes to SIPA. Likewise, SIPA of apyrase-treated platelets was restored upon P2X$_1$ activation with L-β,γ-methylene ATP, which promoted granule centralization within platelets and stimulated P-selectin expression, which is a marker of α-granule release. In addition, during SIPA, platelet degranulation required both extracellular Ca^{2+} and VWF-glycoprotein Ibα interactions without involving $\alpha_{IIb}\beta_3$. Neither platelet release nor SIPA was affected by protein kinase C inactivation, even though protein kinase C blockade inhibits platelet responses to collagen and thrombin in stirring conditions. In contrast, inhibiting myosin light chain (MLC) kinase with ML-7 reduced platelet release and SIPA by 30%. Accordingly, the potentiating effect of P2X$_1$ stimulation on the aggregation of apyrase-treated platelets coincided with intensified phosphorylation of MLC and was abrogated by ML-7. SIPA-induced MLC phosphorylation occurred exclusively through released nucleotides and selective antagonism of P2X$_1$ with MRS2159-reduced SIPA, ATP release, and potently inhibited MLC phosphorylation. We conclude that the P2X$_1$ ion channel induces MLC-mediated cytoskeletal rearrangements, thus contributing to SIPA and degranulation during VWF-triggered platelet activation.

Blood platelets are constantly subjected to hemodynamic forces imposed by the blood flow, including fluid shear stress.

High shear stress is generated at sites of arterial injury where laminar blood flow is forced through a stenosis (1, 2). Shear stress-triggered platelet activation and subsequent aggregation, termed SIPA[1] (3), may thus contribute to the pathogenesis of vascular diseases. In addition, platelets from patients with acute myocardial infarction (4) or cerebral ischemia (5) display enhanced SIPA *in vitro*.

High shear stress is required for the interaction between von Willebrand factor (VWF) and platelet glycoprotein Ibα (GPIbα) (for review, see Ref. 6), but the effects of shear forces on GPIbα signaling are only just beginning to be defined. Downstream effectors that have been implicated in the VWF-dependent activation of $\alpha_{IIb}\beta_3$ include phosphatidylinositol 3-kinase (PI3K) (7), protein kinase C (PKC) (8), Syk, and Src, as well as co-associated immunoreceptor tyrosine-activated motif-containing transmembrane proteins and adaptor proteins (2). A recent study of platelet adhesion to dimeric VWF A1 domain, which recognizes only GPIbα, showed that GPIbα itself can signal to activate $\alpha_{IIb}\beta_3$ through sequential actions of Src kinases, Ca^{2+} oscillations, and PI3K/PKC (9). It has also been proposed that GPIb signals directly as a consequence of its association with structural cytoskeletal proteins (10), among which GPIbα-bound filamin A, filamentous actin cross-linked by α-actinin, vinculin, and talin would directly link the cytoplasmic domain of GPIbα with the β$_3$ tail of $\alpha_{IIb}\beta_3$ (11).

Studies examining SIPA have suggested that VWF primarily stimulates platelet activation through an indirect pathway linked to ADP release (12, 13). These studies have also shown that platelet activation initiated by VWF-GPIbα interaction requires a transmembrane Ca^{2+} influx independent of released ADP and VWF binding to $\alpha_{IIb}\beta_3$ (14, 15), which promotes dense granule secretion of ADP and activates integrin $\alpha_{IIb}\beta_3$ through engagement of the P2 receptors for ADP. A role for the platelet ADP receptors P2Y$_1$ and P2Y$_{12}$ (reviewed in Ref. 16) in SIPA has subsequently been confirmed (17, 18). Reséndiz et al. (19) recently reported that the selective P2Y$_{12}$ antagonist AR-C69931MX inhibits the shear-induced aggregation of washed platelets and showed that P2Y$_{12}$ mediates shear-induced PI3K activation, a process coupled to phosphorylation of PI3K-associated Syk tyrosine kinase.

In blood vessels, shear stress causes the release of high levels of nucleotides, including ATP and ADP, into the extracellular environment; these nucleotides mainly originate from endothelial cells (20) and platelet-dense granules (21). Although the

[1] The abbreviations used are: SIPA, shear-induced platelet aggregation; meATP, methylene ATP; CaM, calmodulin; MLC, myosin light chain; PI3K, phosphatidylinositol 3-kinase; PKC, protein kinase C; VWF, von Willebrand factor; GP, glycoprotein; PAR, protease-activated receptor; TRAP$_{1-6}$, thrombin receptor activating peptide SFFLRN.

shear-induced ATP release from endothelial cells probably involves vesicular exocytosis (22), the molecular mechanisms of such a release are largely unknown. In platelets, the time course of this ATP release appeared to parallel the association of myosin with the actin cytoskeleton, suggesting that these two processes are related (21). In addition, Ca^{2+} influx-dependent phosphorylation of myosin light chain, preceding the myosin-actin interactions, has been proposed to be an initial step during SIPA (21).

ATP is the physiological agonist at P2X₁, but its role in platelet activation is only starting to be unraveled. In the aggregometer, the selective P2X₁ agonists α,β-meATP and L-β,γ-meATP evoke a transient Ca^{2+} influx accompanied by rapid and reversible platelet shape change and myosin light chain (MLC) phosphorylation, provided that measures are taken to avoid desensitization of P2X₁ by ATP spontaneously released during platelet preparation (23–25). Recent studies, using P2X₁ knock-out mice (26) or transgenic mice overexpressing this ion channel selectively in the megakaryocytic cell lineage (27), have reported a prominent role for P2X₁ in platelet aggregation and thrombus formation in shear stress conditions. Notably, P2X₁ overexpressing platelets displayed potent SIPA in conditions where wild-type platelets hardly aggregated (27). In the present study, we have investigated the role of the P2X₁-mediated Ca^{2+} influx and the associated downstream signaling pathways in VWF-dependent shear-induced granule release and aggregation of washed human platelets.

EXPERIMENTAL PROCEDURES

Materials—ADP, L-β,γ-meATP, the P2X₁ antagonist MRS2159, the P2Y₁ antagonist MRS2179, and the ectonucleotidase apyrase (grade I) were purchased from Sigma. AR-C69931MX was a gift from AstraZeneca R&D, Charnwood, UK. The P2X₁ antagonist MRS2159 at the concentration used in this study was verified to selectively inhibit a P2X₁-mediated platelet shape change without affecting platelet shape change and aggregation induced by ADP. The calmodulin inhibitor W-7, the MLC kinase inhibitor ML-7, the Rho kinase inhibitor Y-27632, and the PKC inhibitors GF109203X, Go6976, and Go6983 were purchased from Calbiochem. Human VWF was purified from plasma cryoprecipitate by gel filtration on a Sepharose 4B-CL column. Tirofiban (Aggrastat) was obtained from Merck Sharp and Dohme. The murine-neutralizing anti-VWF monoclonal antibody AJvW-2 was from Ajinomoto Co., Inc. (Kawasaki, Japan) (28), and the neutralizing monoclonal anti-GPIbα antibody G19H10 was raised in our laboratory. ADP and L-β,γ-meATP were purified by high pressure liquid chromatography on an Adsorbosphere HS C18, 7 μm, 250 × 4.6-mm column (Alltech) as described by Oury *et al.* (24).

Preparation of Washed Human Platelets—Washed human platelets ($2.5–3.5 \times 10^5$ platelets/μl) were prepared as described previously (29). Apyrase (0.5 units/ml) was added to the blood sample and platelet resuspension buffer when indicated. Platelet preparations were free of red blood cells, as validated via microscopy and blood cell counting (CellDyn 1300, Abbott, Abbott Park, IL).

Shear-induced Platelet Aggregation, ATP Secretion, and P-selectin Expression—Shear-induced aggregations of washed human platelets were performed in an annular ring-shaped viscometer generating laminar flow (Ravenfield viscometer; Heywood, Lancashire, UK) at 37 °C in the presence of 2 mM CaCl₂ and 10 μg/ml human soluble VWF unless otherwise indicated. A shear rate of 9000 s⁻¹ was used, which corresponds to a shear stress of 80 dynes/cm². The threshold shear rate causing platelet aggregation ranged between 3000 s⁻¹ and 5000 s⁻¹. At defined time points, platelet samples were collected and fixed in 1% paraformaldehyde; the percentage of platelet aggregation was calculated by comparing single platelet counts before and after shearing. Shear-induced P-selectin surface translocation on tirofiban-treated washed platelets was detected by flow cytometry with the phycoerythrin-conjugated anti-P-selectin CD62P antibody (BD Biosciences). For ATP secretion assays, the reactions were stopped with an ice-cold Hepes buffer (20 mM Hepes, pH 7.4, 150 mM NaCl, 5 mM EDTA). After immediate centrifugation at 4 °C, ATP was measured in the supernatants by the addition of a luciferase/luciferin reagent (Chrono-Lume, Kordia) in a microplate luminometer LB96V (Berthold Technologies, Vilvoorde, Belgium). At least five independent experiments were per-

formed on platelets from different individuals. The data are represented as the mean ± S.D. Statistical analysis of the data was done using nonpaired Student's *t* tests.

Immunoblotting Analyses—Platelets (0.3-ml platelet suspensions) were lysed in SDS sample buffer (62.5 mM Tris-HCl, pH 6.8, 2% SDS, 10% glycerol, 50 mM dithiothreitol, 0.1% bromphenol blue). Sample aliquots were loaded on SDS-PAGE (12.5%) and subjected to Western blotting. Thr-18/Ser-19 MLC phosphorylation was detected with the anti-phospho-MLC polyclonal antibody (Santa Cruz Biotechnology, Santa Cruz, CA) according to the instructions of the manufacturers.

Electron Microscopy—Washed platelets were immediately fixed overnight at 4 °C in 2.5% (w/v) glutaraldehyde, 0.1 M phosphate buffer, pH 7.2. After centrifugation at 800 × g for 10 min, a condensed pellet of platelets was formed. After fixation in 1% OsO₄ (w/v), 0.1 M phosphate buffer, pH 7.2, and dehydration in a graded series of ethanol, the pellets were embedded in epoxy resin. Ultrathin sections were cut and stained with uranyl acetate and lead citrate before examination with a Zeiss EM 10 electron microscope (Oberkochen, Germany).

RESULTS

VWF-GPIbα Interactions and Extracellular Ca^{2+} in SIPA—When suspensions of washed human platelets were subjected to uniform high shear stress (80 dynes/cm² = 9000 s⁻¹ shear rate) in the presence of soluble human VWF in an annular ring-shaped viscometer, aggregation rapidly occurred, reaching a plateau after 3 min (Fig. 1*A*). In contrast, a shear rate of 1000 s⁻¹ did not cause platelet aggregation (Fig. 1*A*). The inclusion of the VWF A1 domain-blocking antibody AJvW-2, neutralizing anti-GPIbα antibody G19H10, or the $\alpha_{IIb}\beta_3$ antagonist tirofiban (Fig. 1*B*) confirmed the findings of others (30) that SIPA requires VWF interactions with GPIbα and the activation of $\alpha_{IIb}\beta_3$. We also confirmed that SIPA does not occur in the absence of added extracellular Ca^{2+} (14, 15) (Fig. 1*B*).

Platelet aggregation was accompanied by gradually increasing shear stress-dependent ATP release (Fig. 1*A*). ATP release was initiated as early as 10 s after exposure to shear stress. When measured at the maximal aggregation time point, this release clearly relied on VWF-GPIbα signaling, as it was at least partly inhibited by AJvW-2 and G19H10 (Fig. 1*B*). Omitting the addition of extracellular Ca^{2+} also reduced the amount of released ATP, although only partly (Fig. 1*B*). The combined absence of VWF and extracellular Ca^{2+} almost abolished platelet degranulation (Fig. 1*B*). In contrast, $\alpha_{IIb}\beta_3$ antagonism had no effect on the degree of platelet degranulation (Fig. 1*B*). Therefore, both VWF-GPIbα signaling and Ca^{2+} contribute to platelet release under shear stress, a process that is independent of $\alpha_{IIb}\beta_3$ outside-in signals.

MLC Kinase (but Not PKCs) Controls the SIPA-induced Platelet Degranulation—Platelet granule release that is induced by most agonists requires an increase of intracellular Ca^{2+} and PKC activation (reviewed in Ref. 31). Whether or not PKC plays a role in SIPA is controversial (8, 32). In our experimental conditions, the nonselective PKC inhibitor GF109203X, which blocks both conventional (α, βI, βII, γ) and novel (δ, θ, η, ϵ) PKC isoforms, failed to inhibit either platelet aggregation or release produced by shear stress (Fig. 2*A*), although it prevented such responses to collagen (2 μg/ml) or to the PAR-1-activating peptide TRAP₁₋₆ (1 μM) under stirring conditions (Fig. 2*B*). Similarly, the PKC α/β-specific inhibitor Go6976 did not affect SIPA and associated platelet release (Fig. 2*A*), although shear stress-independent collagen-induced release and aggregation were fully blocked (Fig. 2*B*). In agreement with previous reports that PKC α/β isoforms do not play a major role downstream of PAR-1 (33), Go6976 had a minimal inhibitory effect on TRAP₁₋₆-induced granule release (Fig. 2*B*). Finally, to determine whether other PKC isoforms could be involved in platelet release accompanying SIPA, we used Go6983, which blocks the platelet-expressed atypical PKC ζ isoform in addition to PKC α, βI, βII, γ, and δ. This inhibitor had no effect on shear-induced
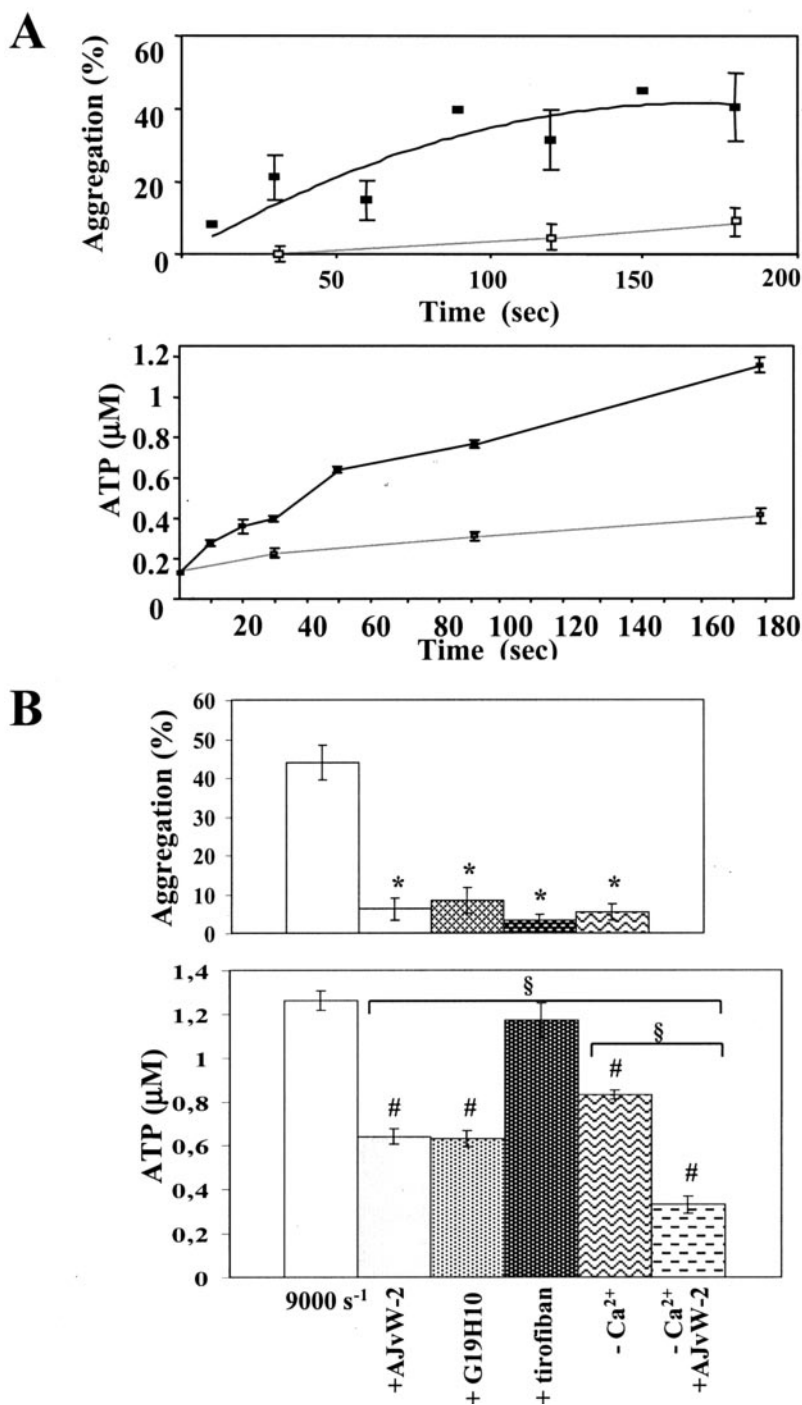
P2X₁ Signaling in SIPA

FIG. 1. **Role of VWF and Ca²⁺ in shear-induced platelet aggregation and ATP release.** *A*, time course of washed human platelet aggregation and ATP release induced at a shear rate of 9000 s⁻¹ (*black squares*). The absence of platelet responses at a shear rate of 1000 s⁻¹ is also shown (*lower lines* with *open squares*). *B*, effects of preincubation with the neutralizing anti-VWF monoclonal antibody AJvW-2 (20 μg/ml, 1 min), the neutralizing anti-GPIbα antibody G19H10 (20 μg/ml, 1 min), or the $\alpha_{IIb}\beta_3$ antagonist tirofiban (1 μg/ml, 1 min), as well as the absence of added extracellular Ca²⁺ on aggregation induced for 3 min at 9000 s⁻¹. *, $p < 0.0001$; #, $p < 0.0001$ *versus* control; §, $p < 0.0002$.

platelet release or aggregation, although it diminished TRAP₁₋₆-induced ATP release by about 50% without affecting platelet aggregation (Fig. 2*B*). These results indicate that shear-induced platelet dense granule release and aggregation are dependent on signaling pathways distinct from those activated downstream of the collagen receptor GPVI or PAR-1. They also suggest that the known conventional, novel, and atypical PKC isoforms do not play a major role in platelet degranulation during SIPA.

In addition to PKC, GPVI-mediated platelet dense granule release also depends on Ca²⁺-sensitive MLC kinase activation (25). Inhibiting this kinase with ML-7 abolished both the ATP release and platelet aggregation induced by collagen (2 μg/ml) (Fig. 2*B*). As shown in Fig. 2*A*, ML-7 reduced the shear-induced ATP release and platelet aggregation by about

30%, indicating a role for MLC kinase in SIPA and associated platelet degranulation.
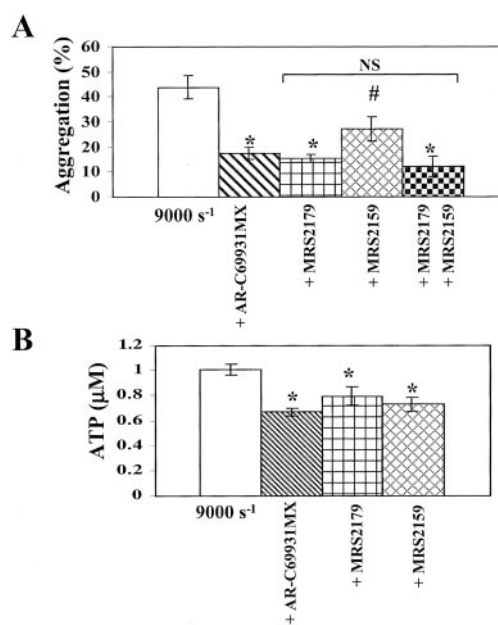
Secreted ADP and ATP in VWF-dependent Shear-induced Platelet Release and Aggregation—Under stirring conditions in an aggregometer, MLC kinase is activated downstream of the P2X₁-mediated Ca²⁺ influx, playing an essential role during cytoskeletal rearrangements evoked by selective agonists (α,β-meATP and L-β,γ-meATP) of this ion channel (25). The activation of MLC kinase can also result from phospholipase C-dependent Ca²⁺ mobilization from internal stores downstream of the G_q protein-coupled P2Y₁ receptor or of GPVI (34, 35). In agreement with earlier reports (17–19), the selective antagonists of P2Y₁ (MRS2179, 10 μM) and P2Y₁₂ (AR-C69931MX, 1 μM) inhibited SIPA by more than 50% (Fig. 3). In previous studies of platelet aggregation performed under stirring conditions in an aggre-
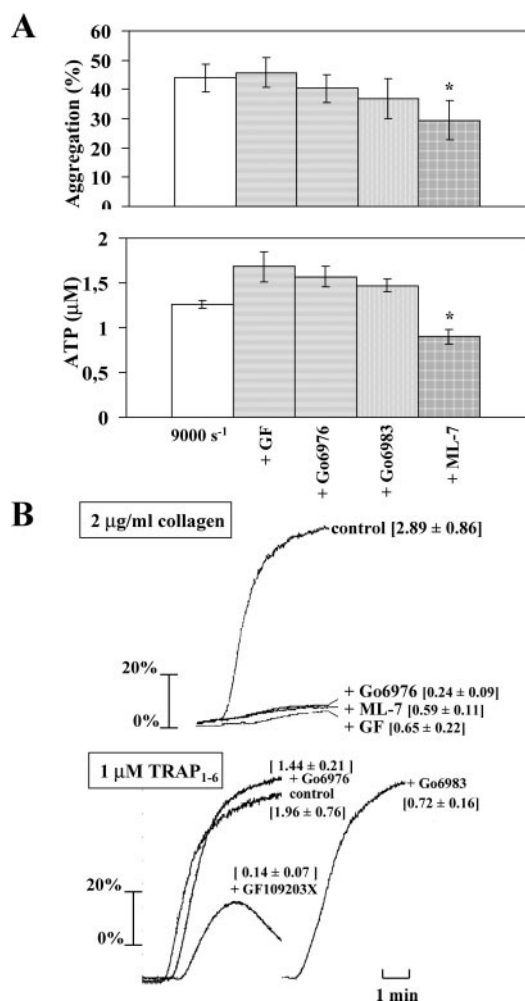
Fig. 2. **MLC kinase *versus* PKC in SIPA and platelet ATP release.** *A*, aggregation of washed human platelets was induced for 3 min at a shear rate of 9000 s^{-1} following preincubation with the protein kinase C inhibitors GF109203X (+*GF*, 10 μM, 5 min), Go6976 (1 μM, 5 min), or Go6983 (1 μM, 5 min) or the MLC kinase antagonist ML-7 (10 μM, 10 min). The effect of these inhibitors on ATP secretion measured after 3 min of shearing is also shown. *, $p < 0.05$. *B*, aggregation of washed human platelets produced in an aggregometer by collagen (2 μg/ml) or TRAP$_{1-6}$ (1 μM SFFLRN) in the absence (*control*) or presence (+) of the same inhibitors, as indicated. The corresponding concentrations (μM) of released ATP are shown in *brackets*.

Fig. 3. **P2X$_1$, P2Y$_1$, and P2Y$_{12}$ in SIPA and ATP release.** *A*, aggregation of washed platelets was induced for 3 min at a shear rate of 9000 s^{-1} following a 1-min preincubation with the selective P2 receptor antagonists for P2Y$_{12}$ (*AR-C69931MX*, 1 μM), P2Y$_1$ (*MRS2179*, 10 μM), and P2X$_1$ (*MRS2159*, 10 μM) or with combined MRS2179 + MRS2159. *, $p < 0.001$; #, $p = 0.04$ *versus* control. *B*, ATP secretion measured after 3 min of shearing in the presence or absence of the P2 receptor antagonists. *, $p < 0.05$; *NS*, not significant.

pretation that these receptors participate in other processes leading to SIPA besides secretion regulation.

P2X$_1$ Enhances Degranulation and SIPA via Calmodulin-dependent MLC Kinase Activation—To further examine the contribution of individual nucleotides to SIPA, we have used platelets of a Hermansky-Pudlak patient lacking dense granules and secreting almost no ATP in response to supraoptimal doses of collagen (36). These platelets displayed severely impaired SIPA comparable with SIPA observed in the presence of P2Y$_1$ or P2Y$_{12}$ receptor antagonists (Fig. 4*A*). Interestingly, platelet aggregation could be largely restored by the addition of not only ADP but also of the selective P2X$_1$ agonist L-β,γ-meATP immediately prior to shearing, which supports the central roles for both ATP and ADP secreted during SIPA.

We pursued this aspect of SIPA using normal platelets but in the presence of the ectonucleotidase apyrase, which degrades secreted ATP and ADP. The addition of apyrase (0.5 units/ml) to the platelet resuspension buffer reduced the level of SIPA to 70% of the control (Fig. 4*B*). In this condition, the selective P2Y$_1$ and P2X$_1$ receptor antagonists MRS2179 and MRS2159 no longer inhibited the remaining SIPA (not shown), indicating that the reduction of aggregation by apyrase is due to the absent activation of P2Y$_1$ and P2X$_1$ signaling (Fig. 4*A*). In contrast, the P2Y$_{12}$ antagonist still reduced the aggregation of apyrase-treated platelets from $26.3 \pm 9.5\%$ to $17.1 \pm 3.2\%$, indicating the presence of sufficient remaining secreted ADP to activate this receptor.

The addition of the selective apyrase-resistant P2X$_1$ agonist L-β,γ-meATP to this set-up just prior to shearing fully restored the aggregation of apyrase-treated platelets (Fig. 4*B*). The resulting aggregation still depended on VWF and $\alpha_{IIb}\beta_3$ activation, as shown by its full inhibition by AJvW-2 and tirofiban (Fig. 4*B*). Therefore, this experimental approach enabled us to study the P2X$_1$-driven signaling pathways in more detail during SIPA.

We found that the enhanced SIPA was the result of CaM and MLC kinase activation, as W-7 and ML-7 inhibited the L-β,γ-

gometer, a high concentration of the ATP/ADP scavenger apyrase always was required to demonstrate P2X$_1$ function, as this ion channel is rapidly desensitized by ATP released during platelet preparation (23–25). In sharp contrast, the P2X$_1$ antagonist MRS2159 (10 μM) reduced SIPA by about 40% even when apyrase was omitted (Fig. 3). Thus, the three platelet P2 receptors contribute to SIPA through secreted ADP and ATP. The effect of combined P2X$_1$ and P2Y$_1$ antagonism on SIPA was not significantly different from that of P2Y$_1$ antagonism only (Fig. 3), suggesting that these receptors share common signaling pathways. Neither the antagonism of P2X$_1$, P2Y$_1$, nor their combination could inhibit the remaining SIPA observed in the presence of the P2Y$_{12}$ antagonist (data not shown).

ATP secretion assays performed in the presence of the selective P2 receptor antagonists revealed a contribution of P2Y$_1$, P2Y$_{12}$, and P2X$_1$ to VWF-dependent platelet degranulation (measured after 3 min) (Fig. 3). With the exception of P2X$_1$ antagonism, the effects of P2Y$_1$ and P2Y$_{12}$ antagonism on secretion did not fully correlate with their ability to inhibit platelet aggregation (Fig. 3), which is in agreement with the inter-

FIG. 4. **P2X₁ activation potentiates SIPA through CaM and MLC kinase.** *A*, SIPA with platelets from a Hermansky-Pudlak patient (*HPS*) compared with platelets from healthy individuals (*control*). L-β,γ-meATP (10 μM) or ADP (1 μM) was added to the Hermansky-Pudlak patient platelets prior to shearing, as indicated. *B*, aggregation of washed platelets and of apyrase (0.5 units/ml)-treated platelets was induced for 3 min at a shear rate of 9000 s^{-1} (*control*) in the presence or in the absence of the selective P2X₁ agonist L-β,γ-meATP (10 μM) following preincubation with the neutralizing anti-VWF monoclonal antibody AJvW-2 (20 μg/ml), the $\alpha_{IIb}\beta_3$ antagonist tirofiban (+*tir*, 1 μg/ml), the CaM antagonist W-7 (100 μM), the MLC kinase antagonist ML-7 (10 μM), or the P2Y₁₂ antagonist AR-C69931MX, as indicated. \$, $p = 0.004$ *versus* control; *, $p = 0.001$ *versus* apyrase − L-β,γ-meATP; **, $p < 0.005$; #, $p < 0.01$ *versus* apyrase + L-β,γ-meATP; ¶, $p = 0.02$ *versus* presence of W-7). The presence of apyrase and L-β,γ-meATP are represented by *solid black lines* underscoring the graph.
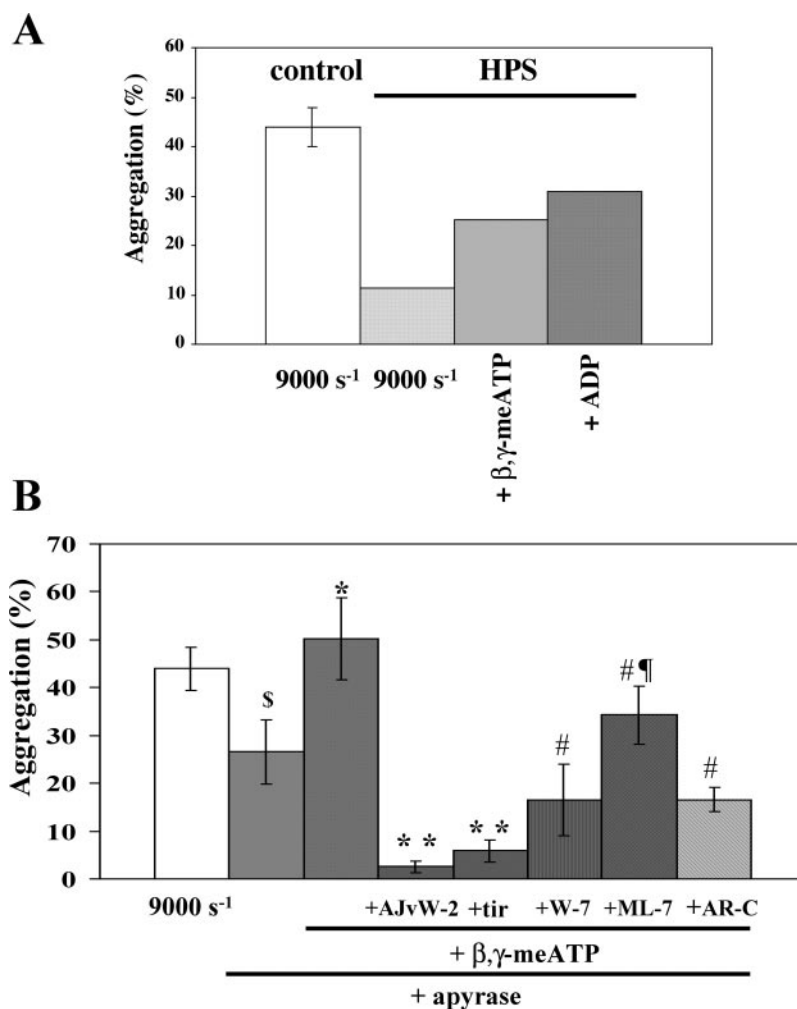
meATP amplification (Fig. 4*B*). Notably, these inhibitors had no effect on the SIPA of apyrase-treated platelets without additional stimulation by L-β,γ-meATP (data not shown), indicating that the activation of these pathways exclusively depends on P2X₁ potentiation. The fact that W-7 inhibited the L-β,γ-meATP-driven SIPA to a larger extent than ML-7 may indicate the existence of an additional CaM-dependent pathway activated downstream of P2X₁. Thus, exogenous P2X₁ activation selectively triggers CaM-dependent pathways contributing to SIPA. Moreover, in the presence of the P2Y₁₂ receptor antagonist AR-C69931MX, the L-β,γ-meATP-driven SIPA was reduced to the same level (16.2 ± 3.4%) as that achieved during inhibition of apyrase-treated platelets themselves, confirming a central role for ADP also in the L-β,γ-meATP-driven SIPA.

P2X₁ Activation Promotes Shear-induced Platelet Granule Centralization and Release—We investigated whether P2X₁-mediated MLC kinase activation would be instrumental in platelet degranulation to explain the enhanced SIPA of Hermansky-Pudlak patient platelets or of apyrase-treated platelets in the presence of L-β,γ-meATP. Flow cytometry analysis of P-selectin expression (as a marker of α-granule release) was done on the surface of apyrase-treated (0.5 units/ml) and tirofiban-treated platelets exposed to VWF and shear for 5 min in the presence or absence of L-β,γ-meATP. Fig. 5 shows a significant increase of the percentage of platelets expressing P-selectin following their pretreatment with L-β,γ-meATP. P-selectin expression was, in turn, reduced to the initial level in the presence of the MLC kinase inhibitor ML-7 (Fig. 5). Therefore, during SIPA, the P2X₁-mediated MLC kinase activation can reinforce the shear-induced platelet degranulation.

The ability of P2X₁ to potentiate platelet aggregation during SIPA was further investigated by electron microscopy of platelet aggregates (Fig. 5). Following 3 min of shearing, the apyrase (0.5 units/ml)-treated platelets formed small aggregates and displayed granule centralization and pseudopodia, but most of the granules were intact (Fig. 5*c*). On the contrary, in the presence of L-β,γ-meATP, larger platelet aggregates were observed in which more platelets were degranulated; in the platelets still showing intact granules, their centralization appeared more advanced than in the absence of L-β,γ-meATP, indicative of more pronounced cytoskeletal rearrangements (Fig. 5*d*). Platelets subject to low shear stress (1000 s^{-1} shear rate) did not show any morphological changes (Fig. 5*b*) as compared with resting platelets (Fig. 5*a*). Thus, P2X₁-driven MLC kinase activation in SIPA contributes both to cytoskeletal rearrangements in platelets and to degranulation.

Shear-induced MLC Phosphorylation Depends on P2X₁, P2Y₁, and P2Y₁₂—Activation of CaM-regulated MLC kinase and Rho kinase results in Ca^{2+}-dependent and -independent phosphorylation of MLC (34), which is a key step in platelet activation. Shear stress caused phosphorylation of MLC (detected as early as 20 s and reaching its maximum after 3 min) (Fig. 6*A*), which was inhibited both by ML-7 and the Rho kinase inhibitor Y-27632 (Fig. 6*B*). Such phosphorylation was not affected by the $\alpha_{IIb}\beta_3$ antagonist tirofiban (Fig. 6*B*), indicating that it occurred independently of $\alpha_{IIb}\beta_3$ outside-in signals. In agreement with a role for Rho kinase in SIPA, platelet aggregation was reduced from 43.9 ± 9.5% to 23.6 ± 8.7% by adding Y-27632 (5 μM) during SIPA (37).

We found that antagonizing P2X₁ (MRS2159), P2Y₁
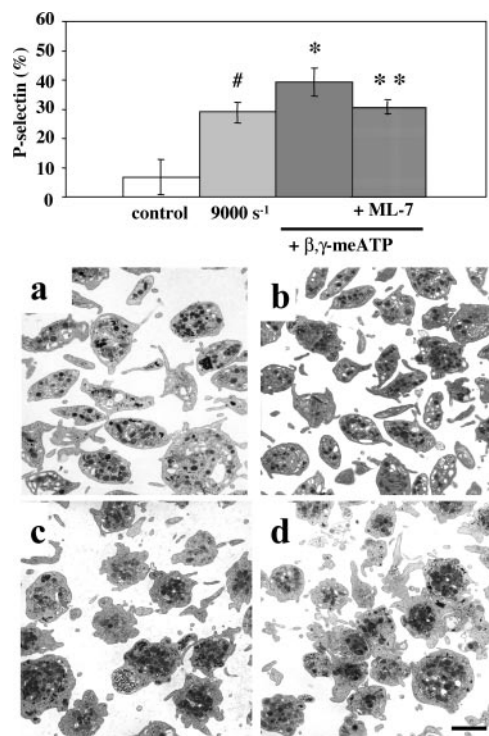
FIG. 5. **P2X₁ activation enhances platelet degranulation.** *Upper panel*, flow cytometry analyses of P-selectin surface expression on tirofiban- and apyrase (0.5 units/ml)-treated washed platelets exposed to VWF at a shear rate of 9000 s⁻¹ for 5 min or not (*control*) in the presence or absence of L-β,γ-meATP (10 μM) and the MLC kinase inhibitor ML-7 (10 μM) as indicated. #, $p = 0.01$ *versus* control; *, $p = 0.02$ *versus* absence of L-β,γ-meATP; **, $p = 0.04$ *versus* presence of L-β,γ-meATP. *Lower panels* (*a–d*), transmission electron microscopy of SIPA. Apyrase (0.5 unit/ml)-treated washed human platelets were subjected or not (*a*) to a shear rate of 1000 s⁻¹ (*b*) or 9000 s⁻¹ (*c*) in the absence or presence of L-β,γ-meATP (10 μM) (*d*) for 3 min before being analyzed by electron microscopy. *Scale bars* = 1 μm.

(MRS2179), or P2Y₁₂ (AR-C69931MX) inhibited phosphorylation of MLC to a variable degree (Fig. 6*B*). Phosphorylation was inhibited potently by P2X₁ neutralization. Correspondingly, the addition of 0.5 units/ml apyrase (*i.e.* abolishing platelet activation via P2Y1 and P2X₁) almost abolished MLC phosphorylation (Fig. 6*C*); moreover, shearing for 20 s resulted in a phosphorylation state below that of resting platelets (Fig. 6*C*). The addition of 5 units/ml apyrase abrogated the overall response (Fig. 6*D*), which could not be restored by doubling the concentration of exogenous VWF (20 μg/ml) (Fig. 6*D*), even though this led to an ~20% increase of aggregation (not shown). Thus, VWF does not trigger MLC phosphorylation without involving secreted nucleotides.

Fig. 6*C* also shows that, in the presence of 0.5 units/ml apyrase, the addition of L-β,γ-meATP prior to shear potently enhanced MLC phosphorylation induced after 20 and 60 s; such L-β,γ-meATP-elicited phosphorylation was quickly reversible as it was no longer detected after 3 min. Therefore, the ability of L-β,γ-meATP to cause MLC phosphorylation coincides with its ability to potentiate the shear-induced aggregation of apyrase-treated platelets.

DISCUSSION

In the present study, we describe a role for the P2X₁-mediated CaM and MLC kinase activation in VWF-dependent SIPA through secreted ATP. This pathway contributes to the extracellular Ca²⁺-dependent platelet degranulation induced by shear stress and acts in conjunction with VWF-GPIbα signaling. As schematically represented in Fig. 7, platelet activation initiated by the VWF-GPIbα interaction required a transmem-
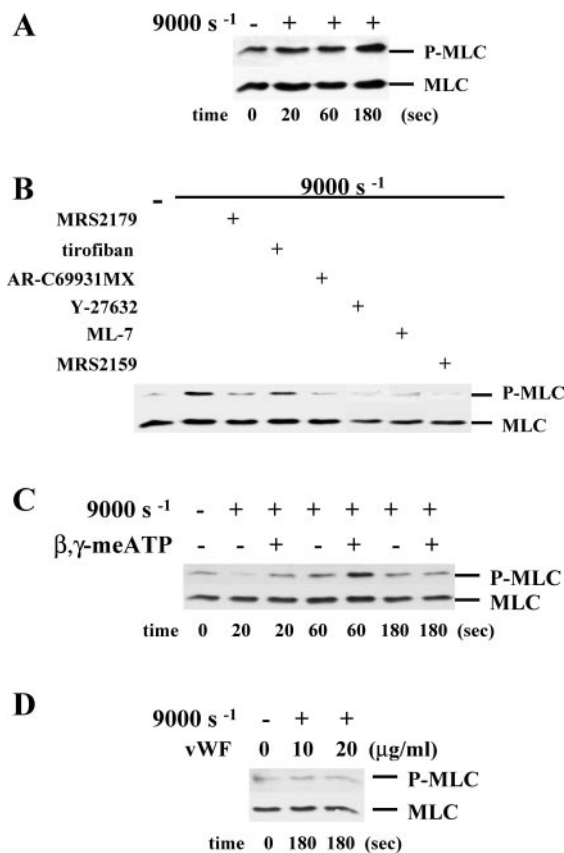

FIG. 6. **Shear-induced MLC phosphorylation depends exclusively on secreted ATP and ADP.** *A*, Western blotting of MLC phosphorylation (*P-MLC*) at a shear rate of 9000 s⁻¹. The time course of MLC phosphorylation in the absence of apyrase is shown. *B*, MLC-phosphorylation produced after 3 min of shear following preincubation with the selective P2 receptor antagonists (as described in the legend for Fig. 3), ML-7 (in Fig. 2), Y-27632 (5 μM), or tirofiban (in Fig. 1*B*), as indicated. *C*, same experiment as in *A* performed on platelets treated with 0.5 units/ml apyrase in the absence or presence of L-β,γ-meATP (10 μM). *D*, platelets were treated with 5 units/ml apyrase, and shear was applied for 3 min in the presence of 10 or 20 μg/ml VWF, as indicated.

brane Ca²⁺ influx independent of both ADP and VWF binding to α$_{IIb}$β₃ (14, 15). Our observation that the P2X₁ receptor antagonist MRS2159 only partly inhibits platelet degranulation and aggregation (to a maximum of 60%), whereas omitting extracellular Ca²⁺ or neutralizing VWF abolishes it, suggests that the VWF/GPIb-associated transmembrane Ca²⁺ influx only partly relies on P2X₁-mediated Ca²⁺ influx.

In contrast to the effects on aggregation, the removal of VWF or antagonizing its binding to GPIbα only partially reduced the shear-induced platelet ATP release unless extracellular Ca²⁺ was omitted at the same time. The antagonist of α$_{IIb}$β₃, tirofiban, had no effect on shear-induced platelet release, excluding contributions by VWF-α$_{IIb}$β₃ outside-in signaling to secretion regulation. Antagonizing P2X₁ with MRS2159 diminished the ATP release, which was also seen with the antagonism of P2Y₁ and P2Y₁₂, indicating a role for all of these receptors in the amplification of the VWF/GPIbα-triggered platelet degranulation (Fig. 7).

The ATP-gated P2X₁ ion channel only operates in the presence of physiological extracellular Ca²⁺ concentrations (23, 24). Ca²⁺ is a key element in granule secretion (reviewed in Ref. 31). The proteins that mediate the effects of Ca²⁺ in secretion fall into two categories: the EF hand proteins and the Ca²⁺/phospholipid-binding proteins. EF hand proteins found in platelets include calmodulin and calcyclin. Calmodulin binds to platelet α-granules. Ca²⁺/calmodulin-dependent phosphorylation of MLC ki-
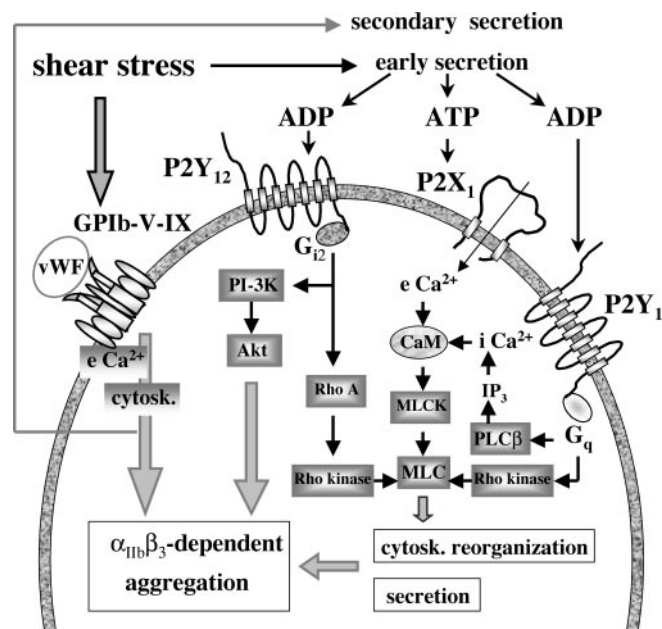
FIG. 7. **Schematic representation of the central role of P2 receptor signaling in SIPA.** In addition to the shear-induced interaction of VWF with GPIbα, a role for all three P2 receptors is depicted in SIPA. Extracellular Ca^{2+}-dependent GPIbα signaling triggers cytoskeletal rearrangements and $\alpha_{IIb}\beta_3$ activation but also early degranulation leading to subsequent activation of P2 receptors via released ADP and ATP. Downstream P2 receptor pathways include P2Y₁-mediated Ca^{2+} mobilization and P2X₁-mediated Ca^{2+} influx, as well as P2Y₁₂-dependent PI3K and Akt activation and RhoA/Rho kinase activation. The three P2 receptors are needed to cause MLC phosphorylation through CaM/MLC kinase and/or RhoA/Rho kinase pathways, leading to shear-associated cytoskeletal reorganization, facilitating platelet aggregation and enhancing platelet secretion. The fast ATP-activated Ca^{2+} influx through P2X₁ triggers rapid CaM activation, which is critical for a process requiring a prompt platelet-activating signal. eCa^{2+} and iCa^{2+}, extracellular and intracellular Ca^{2+}, respectively.

nase mediates secretion via activation of MLC with subsequent contraction of the actomyosin; therefore, the concurrent centralization of granules is thought to facilitate granule secretion (38). Calmodulin may also bind specifically to the vesicle-associated membrane protein (39), contributing to granule release by directly affecting the exocytotic core complex.

Here, we found that shear-induced MLC phosphorylation involves both Ca^{2+}-dependent MLC kinase and Ca^{2+}-independent Rho kinase signaling, as it was inhibited by the MLC kinase inhibitor ML-7 as well as by the Rho kinase inhibitor Y-27632. The phosphorylation of MLC was abolished by the ATP/ADP scavenger apyrase and was potently reduced by the selective antagonism of P2X₁, P2Y₁, or P2Y₁₂, indicating a central role for secreted ATP and ADP in this event.

Compatible with a prominent role for the P2X₁ ion channel under high shear stress (26, 27), apyrase was not needed to demonstrate P2X₁ function during SIPA. On the other hand, apyrase could be used under these conditions to control P2X₁ function via the addition of stable selective P2X₁ agonists and to drive platelet activation through P2X₁-dependent pathways of signaling. The ability of the selective P2X₁ agonist L-β,γ-meATP to restore the aggregation of apyrase-treated platelets coincided with its potency in causing early phosphorylation of MLC and increased platelet P-selectin expression, a marker of α-granule release. The potentiating effect of L-β,γ-meATP on SIPA was prevented by inhibitors of CaM (W-7) and of MLC kinase (ML-7). These findings were substantiated by electron microscopy analyses of the platelet aggregates, depicting more pronounced granule centralization as well as degranulation in the presence of L-β,γ-meATP. Our observation that exogenous

P2X₁ activation can restore the severely defective SIPA of platelets lacking dense granules (Hermansky-Pudlak patient) corroborates a role for P2X₁-mediated cytoskeletal rearrangements in facilitating α-granule release.

Thus, our findings suggest that P2X₁ participates in the extracellular Ca^{2+}-dependent shear-induced platelet granule release through CaM and MLC kinase-triggered MLC phosphorylation and concurrent cytoskeletal rearrangements, facilitating SIPA and leading to granule centralization as an onset to degranulation (Fig. 7). Because P2Y₁ antagonism also inhibited shear-induced MLC phosphorylation (although weakly), a role for Ca^{2+} mobilized from internal stores in MLC kinase activation is possible (34, 35). Rapid P2X₁ and slower P2Y₁ signals (activated by co-released ATP and ADP, respectively) converge to a common effector (MLC kinase) contributing to cytoskeleton remodeling and platelet release (Fig. 7). Accordingly, combined P2X₁ and P2Y₁ antagonism leads to the same inhibition of SIPA at 3 min as P2Y₁ antagonism only.

The study by Schoenwaelder *et al.* (37) defines an important role for RhoA and Rho kinase in SIPA but not in platelet release. The inhibition of shear-induced MLC phosphorylation by selective P2Y₁ or P2Y₁₂ antagonism suggests that ADP activates Rho kinase through G_q (40) and $G_i\alpha_2$ (41) also under shear stress (Fig. 7). Further investigations are required to determine the function of these pathways during SIPA. The failure of Rho kinase inhibitors to affect platelet release (Ref. 37 and the present study) may be explained by the existence of two pools of myosin present in different cell compartments (42) and emphasizes the role of MLC kinase activation in nucleotide-mediated granule release. In agreement with findings by Reséndez *et al.* (19), we further found that P2Y₁₂ mediated PI3K activation during SIPA. The resulting Akt (protein kinase B) phosphorylation was inhibited by P2Y₁₂ neutralization. PI3K inhibition partially inhibited SIPA but had no effect on ATP release (not shown); *i.e.* P2Y₁₂-recruited PI3K activates platelets via a separate pathway (Fig. 7) potentially by regulating the function of $\alpha_{IIb}\beta_3$ via Akt and the integrin-linked kinase ILK (43).

Platelet granule release induced by most platelet agonists depends on PKC activation (reviewed in Ref. 31). However, none of the PKC inhibitors used in this study affected the shear-induced platelet release or aggregation. The nonselective PKC inhibitor GF109203X (which blocks both diacylglycerol- and Ca^{2+}-sensitive conventional PKC isoforms and the diacylglycerol-sensitive Ca^{2+}-insensitive novel isoforms), the more potent PKC α/β-specific inhibitor Go6976, and Go6983 (which inhibits the atypical ζ isoform in addition to α, β, γ, and δ) were all without effect, even though they inhibited platelet release in response to collagen or TRAP₁₋₆. This finding is consistent with a previous study in which the nonselective protein kinase inhibitor staurosporine failed to inhibit SIPA (32). This is in contrast to the study by Kroll *et al.* (8) showing inhibition of the full aggregation response by the staurosporine analogue Ro 31-7549. The effect of this inhibitor on platelet release was not reported in their study. Ro 31-7549, similar to Ro 31-8220 and GF109203X, belongs to a category of nonselective PKC inhibitors showing similar potency in inhibiting collagen-, thromboxane A_2 analogue-, and thrombin-induced platelet release and aggregation (29, 33, 44). These authors show that SIPA is associated with the phosphorylation of pleckstrin, a PKC substrate that occurs in the absence of diacylglycerol or hydrolysis of phosphatidylinositol 4,5-bisphosphate in a Ca^{2+}-dependent manner. It has to be noticed that EGTA, a chelator of extracellular Ca^{2+}, had minimal effect on such phosphorylation, excluding a role for transmembrane Ca^{2+} influx. They conclude that a diacylglycerol-independent pathway of PKC activation

contributes to SIPA. Thus, although involvement of an unknown PKC isoform in shear-induced platelet granule release cannot be ruled out, our data clearly distinguished this process from the GPVI- and PAR-1-mediated granule release (33). Finally, the study by Nakai *et al.* (21) describes the shear-induced cytoskeleton translocation of actin, actin-binding protein, and myosin as a rapid and transient movement of MLC kinase wherein the amount of cytoskeletal PKC did not change, unlike what is seen with thrombin. This observation further suggests distinct roles of PKC (if any) and MLC kinase during platelet responses to shear stress. The transient association of MLC kinase with the cytoskeleton may coincide with the quickly reversible MLC phosphorylation produced via $P2X_1$ activation.

In conclusion, $P2X_1$ contributes to SIPA through its ability to rapidly elicit Ca^{2+} influx-triggered signals leading to prompt CaM-dependent signaling, platelet activation, and platelet granule release. Further studies are required to elucidate the mechanisms of VWF-GPIbα-dependent platelet granule release. It also remains to be determined whether the presently identified $P2X_1$/CaM/MLC kinase pathway plays a role during platelet activation processes accompanying platelet recruitment and adhesion on immobilized VWF and, most importantly, during thrombosis.

REFERENCES

1. Kroll, M. H., Hellums, J. D., McIntire, L. V., Schafer, A. I., and Moake, J. L. (1996) *Blood* **88,** 1525–1541
2. Berndt, M. C., Shen, Y., Dopheide, S. M., Gardiner, E. E., and Andrews, R. K. (2001) *Thromb. Haemostasis* **86,** 178–188
3. Ikeda, Y., Murata, M., and Goto, S. (1997) *Ann. N. Y. Acad. Sci.* **811,** 325–336
4. Goto, S., Sakai, H., Goto, M., Ono, M., Ikeda, Y., Handa, S., and Ruggeri, Z. M. (1999) *Circulation* **99,** 608–613
5. Konstantopoulos, K., Grotta, J. C., Sills, C., Wu, K. K., and Hellums, J. D. (1995) *Thromb. Haemostasis* **74,** 1329–1334
6. Ruggeri, Z. M. (2003) *Curr. Opin. Hematol.* **10,** 142–149
7. Yap, C. L., Anderson, K. E., Hughan, S. C., Dopheide, S. M., Salem, H. H., and Jackson, S. P. (2002) *Blood* **99,** 151–158
8. Kroll, M. H., Hellums, J. D., Guo, Z., Durante, W., Razdan, K., Hrbolich, J. K., and Schafer, A. I. (1993) *J. Biol. Chem.* **268,** 3520–3524
9. Kasirer-Friede, A., Cozzi, M. R., Mazzucato, M., De Marco, L., Ruggeri, Z. M., and Shattil, S. J. (2004) *Blood* **103,** 3403–3411
10. Christodoulides, N., Feng, S., Resendiz, J. C., Berndt, M. C., and Kroll, M. H. (2001) *Thromb. Res.* **102,** 133–142
11. Feng, S., Reséndiz, J. C., Lu, X., and Kroll, M. H. (2003) *Blood* **102,** 2122–2129
12. Moritz, M. W., Reimers, R. C., Baker, R. K., Sutera, S. P., and Joist, J. H. (1983) *J. Lab. Clin. Med.* **101,** 537–544
13. Moake, J. L., Turner, N. A., Stathopoulos, N. A., Nolasco, L., and Hellums, J. D. (1988) *Blood* **71,** 1366–1374
14. Chow, T. W., Hellums, J. D., Moake, J. L., and Kroll, M. H. (1992) *Blood* **80,** 113–120
15. Ikeda, Y., Handa, M., Kamata, T., Kawano, K., Kawai, Y., Watanabe, K., Kawakami, K., Sakai, K., Fukuyama, M., Itagaki, I., Yoshioka, A., and Ruggeri, Z. M. (1993) *Thromb. Haemostasis* **69,** 496–502
16. Kunapuli, S. P., Dorsam, R. T., Kim, S., Quinton, T. M. (2003) *Curr. Opin. Pharmacol.* **3,** 175–180
17. Goto, S., Tamura, N., Eto, K., Ikeda, Y., and Handa, S. (2002) *Circulation* **105,** 2531–2536
18. Turner, N. A., Moake, J. L., and McIntire, L. V. (2001) *Blood* **98,** 3340–3345
19. Reséndiz, J. C., Feng, S., Ji, G. A., Francis, K. A., Berndt, M. C., and Kroll, M. H. (2003) *Mol. Pharmacol.* **63,** 639–645
20. Bodin, P., Bailey, D., and Burnstock, G. (1991) *Br. J. Pharmacol.* **103,** 1203–1205
21. Nakai, K., Hayashi, T., Nagaya, S., Toyoda, H., Yamamoto, M., Shiku, H., Ikeda, Y., and Nishikawa, M. (1997) *Life Sci.* **60,** 181–191
22. Bodin, P., and Burnstock, G. (2001) *J. Cardiovasc. Pharmacol.* **38,** 900–908
23. Rolf, M. G., Brearley, C. A., and Mahaut-Smith, M. P. (2001) *Thromb. Haemostasis* **85,** 303–308
24. Oury, C., Toth-Zsamboki, E., Thys, C., Tytgat, J., Vermylen, J., and Hoylaerts, M. F. (2001) *Thromb. Haemostasis* **86,** 1264–1271
25. Toth-Zsamboki, E., Oury, C., De Vos, R., Vermylen, J., and Hoylaerts, M. F. (2003) *J. Biol. Chem.* **278,** 46661–46667
26. Hechler, B., Lenain, N., Marchese, P., Vial, C., Heim, V., Freund, M., Cazenave, J. P., Cattaneo, M., Ruggeri, Z. M., Evans, R., and Gachet, C. (2003) *J. Exp. Med.* **198,** 661–667
27. Oury, C., Kuijpers, M. J. E., Toth-Zsamboki, E., Bonnefoy, A., Danloy, S., Vreys, I., Feijge, M. A., De Vos, R., Vermylen, J., Heemskerk, J. W. M., and Hoylaerts, M. F. (2003) *Blood* **101,** 3969–3976
28. Kageyama, S., Yamamoto, H., Nagano, M., Arisaka, H., Kayahara, T., and Yoshimoto, R. (1997) *Br. J. Pharmacol.* **122,** 165–171
29. Oury, C., Toth-Zsamboki, E., Vermylen, J., and Hoylaerts, M. F. (2002) *Blood* **100,** 2499–2505
30. Ikeda, Y., Handa, M., Kawano, K., Kamata, T., Murata, M., Araki, Y., Anbo, H., Kawai, Y., Watanabe, K., Itagaki, I., Sakai, K., and Ruggeri, Z. M. (1991) *J. Clin. Investig.* **87,** 1234–1240
31. Flaumenhaft, R. (2003) *Arterioscler. Thromb. Vasc. Biol.* **23,** 1152–1160
32. Oda, A., Yokoyama, K., Murata, M., Tokuhira, M., Nakamura, K., Handa, M., Watanabe, K., and Ikeda, Y. (1995) *Thromb. Haemostasis* **74,** 736–742
33. Murugappan, S., Tuluc, F., Dorsam, R. T., Shankar, H., and Kunapuli, S. P. (2004) *J. Biol. Chem.* **279,** 2360–2367
34. Bauer, M., Retzer, M., Wilde, J. I., Maschberger, P., Essler, M., Aepfelbacher, M., Watson, S. P., and Siess, W. (1999) *Blood* **94,** 1665–1672
35. Paul, B. Z., Daniel, J. L., and Kunapuli, S. P. (1999) *J. Biol. Chem.* **274,** 28293–28300
36. Zhang, Q., Zhao, B., Li, W., Oiso, N., Novak, E. K., Rusiniak, M. E., Gautam, R., Chintala, S., O'Brien, E. P., Zhang, Y., Roe, B. A., Elliott, R. W., Eicher, E. M., Liang, P., Kratz, C., Legius, E., Spritz, R. A., O'Sullivan, T. N., Copeland, N. G., Jenkins, N. A., and Swank, R. T. (2003) *Nat. Genet.* **33,** 145–153
37. Schoenwaelder, S. M., Hughan, S. C., Boniface, K., Fernando, S., Holdsworth, M., Thompson, P. E., Salem, H. H., and Jackson, S. P. (2002) *J. Biol. Chem.* **277,** 14738–14746
38. Painter, R. G., and Ginsberg, M. H. (1984) *Exp. Cell Res.* **155,** 198–212
39. Quetglas, S., Leveque, C., Miquelis, R., Sato, K., and Seagar, M. (2000) *Proc. Natl. Acad. Sci. U. S. A.* **97,** 9695–9700
40. Vogt, S., Grosse, R., Schultz, G., and Offermans, S. (2003) *J. Biol. Chem.* **278,** 28743–28749
41. Liu, F., Verin, A. D., Wang, P., Day, R., Wersto, R. P., Chrest, F. J., English, D. K., and Garcia, J. G. (2001) *Am. J. Respir. Cell Mol. Biol.* **24,** 711–719
42. Burridge, K., Chrzanowska-Wodnicka, M., and Zhong, C. (1997) *Trends Cell Biol.* **7,** 342–347
43. Pasquet, J. M., Noury, M., and Nurden, A. T. (2002) *Thromb. Haemostasis* **88,** 115–122
44. Paul, B. Z., Jin, J., and Kunapuli, S. P. (1999) *J. Biol. Chem.* **274,** 29108–29114